Comparative Cancer Cytogenetics

Nicole McNeil, Cristina Montagna, Michael J. Difilippantonio and Thomas Ried

Center for Cancer Research, Genetics Branch, National Cancer Institute,
National Institutes of Health, Bethesda, MD 20892

It has long been appreciated that tumor cells carry chromosomal aberrations (1). Deviation from the paired ordering of autosomes and sex chromosomes by either increasing or decreasing the copy number of a given chromosome, is referred to as aneuploidy. Errors in the faithful segregation of chromosomes during mitotic or meiotic cell division play a crucial role in the generation of chromosomal aneuploidies, the genetic consequences of which are increased copy numbers of oncogenes and loss of tumor suppressor genes. Cytogenetic abnormalities that affect the integrity of a chromosome are referred to as structural aberrations. These can be either balanced (i.e., no net gains or loss of DNA as in peri- or paracentric inversions and reciprocal translocations) or unbalanced translocations, including duplications, deletions, and non-reciprocal translocations (2). In particular, balanced chromosomal translocations are frequently observed and considered pathogenetic events in haematopoietic malignancies (2-6).

One outcome of a translocation is the re-positioning of an oncogene in proximity to a strong enhancer from another gene. This results in overexpression of the oncogene and can lead to cellular transformation. In human Burkitt's Lymphoma, mouse plasmacytomas and pro-B cell lymphomas, the c-myc oncogene is juxtaposed to the enhancer for the immunoglobulin heavy chain gene (1, 7, 8). Dysregulation of c-myc in this manner is believed to increase both the rate of cell division and chromosome instability (9). Balanced chromosomal translocations can have oncogenic effects through the production of fusion proteins. For instance, in almost 95% of chronic myelogenous leukemia (CML) case a translocation between chromosomes 9 and 22 results in the formation of what is commonly referred to as the Philadelphia chromosome. This results in the fusion of the BCR and ABL genes. The BCR-ABL fusion protein has increased

tyrosine kinase activity and transforms haematopoietic cells (10). Inhibition of the constitutive kinase activity with the BCR-ABL-specific inhibitor STI571 is currently in clinical trials and the overall response rate of patients in blast crisis in one study was reported to be 55%, with complete remission in 11% of the patients (11).

Karyotype analysis based on G- or R-banding techniques have been widely applied to the characterization of cytogenetic abnormalities in tumor cells and have contributed significantly to the identification of recurrently involved chromosomal loci and hence to the molecular cloning of cancer causing genes. In many instances, however, the cytogenetic analysis of chromosomes from solid tumors has proven to be challenging. This is due to the often-low mitotic index, the poor quality of metaphase chromosomes, and the sheer number of cytogenetic abnormalities (12). The use of genetically engineered mice as model systems of human cancer has fueled the need for better cytogenetic analysis in this species as well. Mouse chromosomes do not vary much in size and all are acrocentric. Therefore, some of the parameters used for identification of human chromosomes are less helpful, making karyotyping very difficult. A further drawback at present is that rather few cytogeneticists are trained in karyotyping mouse chromosomes.

The ability to microscopically visualize the location of individual sequences on metaphase chromosomes using fluorescence in situ hybridization (FISH) techniques has greatly broadened the application of cytogenetic methodologies, ushering in the era of molecular cytogenetics (for historical review (13)). FISH probes come in many varieties. They can be specific to (A) unique regions and genes, (B) repetitive sequences such as telomeres and centromeres, (C) entire chromosomes, chromosome bands or arms and (D) in the case of comparative genomic hybridization (CGH) as large as entire genomes. Advances in fluorochrome chemistry (i.e. stability, stoke shift, quantum yield, and conjugability to nucleotides) and photodetection devices (i.e., charged coupled device cameras and photomultiplier tubes) have further enhanced the sensitivity and multiplicity of FISH.

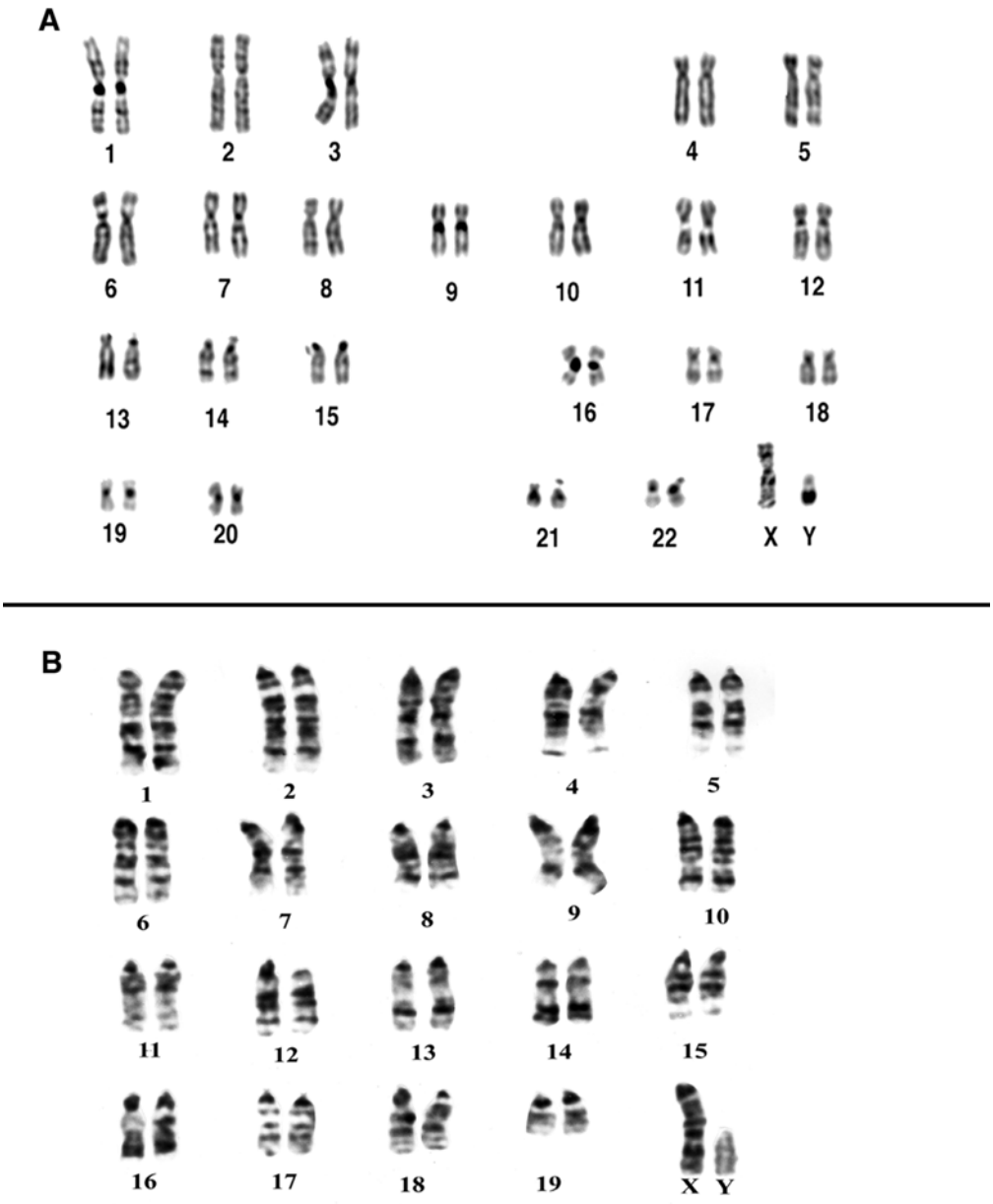

Figure 1: Giemsa staining of chromosomes yields banding patterns.

(A) Human chromosomes come in pairs, one being maternal and the other paternal in origin. They are arranged on the basis of their size and the position of the centromere, or primary constriction. Most human chromosomes contain two arms. The p-arm is shorter and is oriented above the centromere while the q-arm is below the centromere. The normal complement of chromosomes in a human cell is 46. This karyotype is from a male cell as determined by the presence of both an X and Y chromosome. (B) Mouse chromosomes are also organized according to their size, however all of the chromosomes are acrocentric (having the centromere close to one end and thus no p-arm), making karyotyping more of a challenge.

The merging of these technical advances is reflected in the combinatorial labeling and hybridization techniques known as comparative genomic hybridization (CGH) (14), spectral karyotyping (SKY) (15, 16), and m-FISH (17, 18). CGH is a quantitative method for comparing the copy number of genomic regions between a control (DNA extracted from karyotypically normal cells) and test sample (i.e. tumor DNA). SKY and m-FISH involve the hybridization of differentially labeled chromosome painting probes for the identification of both numerical and structural aberrations in the genome. Each of these two conceptual methodologies alone provides a significant advance in the way we analyze genomes. Together, SKY, m-FISH and CGH offer novel tools to understand tumor specific and stage specific chromosome aberrations. In this chapter we provide some Deep Insights into the applications, uses, advantages and limitations of Spectral Karyotyping and Comparative Genomic Hybridization. We will also discuss how these two techniques are being applied to the classification, diagnosis, prognosis and understanding of the cellular mechanisms that lead to cellular transformation.

Spectral Karyotyping

Spectral karyotyping (SKY) is a molecular cytogenetic technique used to generate a color-coded karyotype of human and mouse chromosomes (15, 16). Prior to its development, cytogeneticists analyzed tumors and leukemias using a Giemsa staining technique that produced a dark and light banding pattern on chromosomes (Figure 1). As previously mentioned, chromosomal analysis using this technique alone can be challenging since tumor metaphase chromosomes are often poorly spread, have many rearrangements and subtle translocations or insertions. In combination with chromosome banding techniques, SKY allows for a more comprehensive description of cytogenetic abnormalities (Figure 2) (19).

Spectral karyotyping involves the simultaneous hybridization of 24 chromosome-specific painting probes (Figure 2A). High-resolution, bi-variate flow sorting is first used to isolate each individual normal chromosome on the basis of its size, and A-T vs. G-C content (20). The source of the chromosomes are suspensions prepared from normal human or mouse cells, from cell lines with specific chromosomal rearrangements, human-hamster or mouse-hamster hybrid cell lines, and cell lines from different mouse

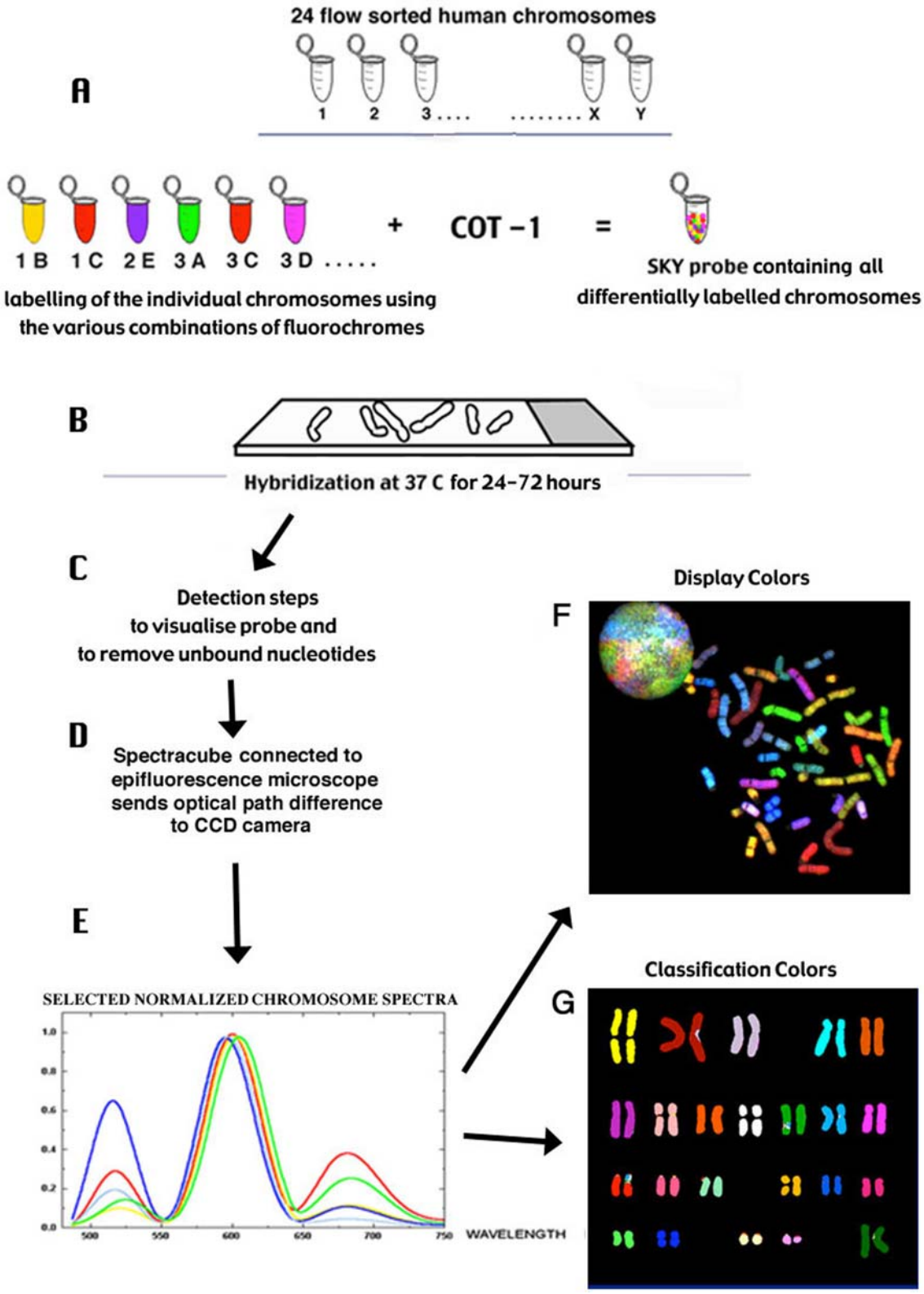

Figure 2: Schematic representation of the steps involved in SKY analysis.

(A) The process begins with the isolation of each individual chromosome by flow sorting. Each chromosome is then labeled with between 1 and 5 fluorochromes (combinatorial labeling) to create a unique spectral signature for each chromosome pair. Aliquots of the painted chromosomes are subsequently pooled together with an excess of Cot-1 DNA necessary to suppress the hybridization of labeled repetitive sequences common throughout the genome.
(B) Both the SKY probe set and the chromosomes to be analyzed are heat denatured prior to hybridization for a 24-72 hour period at 37°C.
(C) Unhybridized probe is removed by increasingly stringent washes. Detection of the non-fluorescently labeled probes is accomplished through the use of fluorescence-conjugated antibodies against the haptens biotin and digoxigenein.
(D) The slide is illuminated with a Xenon lamp in order to simultaneously excite all of the fluorescent dyes. Thefluorescence emitted from the dyes then passes through a custom-designed triple bandpass optical filter to a Sagnac interferometer where an optical path difference is generated for each pixel. The emission spectra from each pixel is finally captured by a CCD camera and transmitted to the acquisition software.
(E) Fourier transformation recovers the spectrum from this interferogram and assigns red, green, and blue (RGB) colors based on the wavelengths of the fluorescence intensities.
(F) The result of the RGB assignment is the visualization of each chromosome as a unique spectral color.
(G) Specialized analysis software then assigns an artificial classification color to each chromosome and places them into a karyotype. This is based on a classification table indicating which dye combinations were used for labeling of the chromosomes in Step A.

strains. These combinations are necessary to assure the flow sorting of pure chromosomes. The DNA from each chromosome is then amplified by a degenerate oligo-primed polymerase chain reaction (DOP-PCR) (21). Next, each chromosome is labeled with either one or a combination of fluorochromes. Using such a combinatorial labeling scheme with five different fluorochromes, 31 different targets can be distinguished. The combinatorial fluorescent labeling produces a unique spectral signature for each chromosome, thereby allowing the simultaneous discernment of all human or mouse chromosomes. After labeling, the chromosome painting probes are pooled together with an excess of Cot-1 DNA to suppress repetitive sequences within the genome and are hybridized onto metaphase chromosomes prepared from the sample of interest (i.e. tumor cells). Following incubation at 37°C for 24-72 hours, residual probe is removed by various stringency washes and subsequent detection steps allow visualization of fluorochromes. Note that only three direct fluorochromes are involved and that the biotin and digoxigenin labeled probes require detection with avidin conjugates or immunological detection (Figures 2B and 2C).

Spectral images are acquired using an interferometer connected to a CCD camera. The fluorochromes are excited by light emitted from a Xenon lamp passing through a custom-made triple-band pass optical filter. The light emitted from the sample (i.e. the fluorescence) is collected by the microscope objective and transferred to a Sagnac interferometer within the head of the Spectral Cube (Applied Spectral Imaging, Carlsbad, CA), which creates an optical path difference (16, 22) (Figure 2D). Fourier transformation resolves the resulting interferogram to a spectrum (Figure 2EF). Next, the spectral signature measured at each pixel is converted to a color code for visualization (Figure 2F). The classification colors are unique colors given to all chromosomes (pixels) that have the same spectrum (Figure 2G).

SKY has greatly enhanced the ability to analyze complex karyotypes from both human tumors and murine model systems. The wide application of SKY has clearly shown that, in combination with banding analyses, complex karyotypes can be resolved with unprecedented accuracy (for a reviews see (23, 24)).

Comparative Genomic Hybridization

Comparative Genomic Hybridization (CGH) employs two-color fluorescence *in situ* hybridization of both tumor DNA and normal control DNA (also known as reference DNA) to normal metaphase chromosomes (25). This molecular cytogenetic technique measures the genetic imbalances within tumor genomes, and has become an exceedingly valuable tool for the analysis of chromosomal aberrations in solid tumors and haematological malignancies (26, 27)**.** One major advantage of CGH is that only genomic tumor DNA is needed for analysis. Therefore, DNA extracted from archived, fixed tumors (28) as well as from microdissected tissue (29) can be analyzed.

After extraction of test DNA (i.e. from a tumor sample) and normal DNA (i.e. from peripheral blood), the samples are differentially labeled with discernable fluorochromes (i.e. tumor DNA with FITC [green] and control DNA with TRITC [red]) (Figure 3A). The two genomes are combined with an excess of human Cot-1 DNA and then hybridized to normal metaphase chromosomes (Figure 3B). Images of metaphase spreads are then acquired with a (charged coupled device) CCD camera and fluorochrome-specific optical filter sets to capture the FITC and TRITC fluorescence

(Figure 3C). Differences in fluorescence intensity values between tumor and control DNA represent gains and losses of specific chromosomes or chromosomal regions (30).

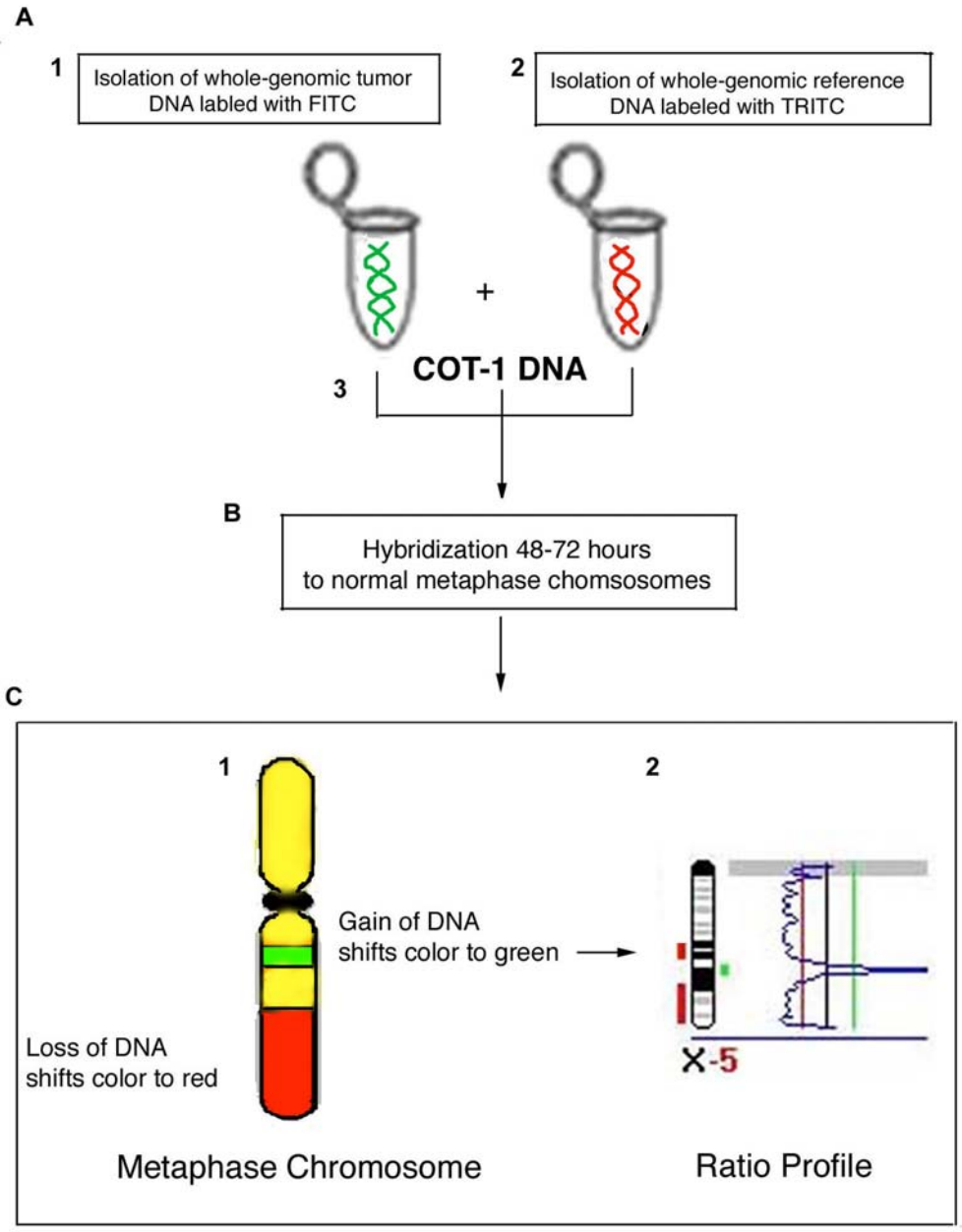

Figure 3: Schematic representation of Comparative Genomic Hybridization.

(A) CGH begins with the isolation of both (1) genomic tumor DNA and (2) DNA from an individual with a normal karyotype (reference or control DNA). The two genomes are differentially labeled such that, for instance, the tumor DNA can be detected with a green fluorochrome (FITC) and the control DNA with a red fluorochrome (TRITC). (3) The differentially labeled genomes are then combined in the presence of excess Cot-1 DNA.

(B) Both the probe and karyotypically normal target metaphase chromosomes are heat denatured prior to hybridization for a 24-72 hour period at 37°C.
(C) Following a series of detection steps, metaphase chromosomes are imaged by epifluorescence microscopy with DAPI, FITC and TRITC filters consecutively.

(1) The differences in fluorescence intensities along a chromosome are a reflection of the actual copy number changes in the tumor genome relative to the normal reference. The result of the hybridization shows gains and losses; in the event that a specific chromosome region is lost in the tumor, the color of that region is shifted to red. A gain would be represented by an increased intensity of the green fluorescence. (2) A minimum of 5 metaphases (or 10 copies of each chromosome) are analyzed to determine an average ratio profile. A ratio of 1 represents an equal copy number in the tumor and the reference genome. The vertical lines to the left and right of the chromosome represent a loss (< 0.8) and a gain (>1.2), respectively.

For example, a gain of a chromosomal region in the test sample would result in an increased intensity of green fluorescence. A loss within a chromosomal region in the tumor would be indicated by a shift towards red intensities. Specialized CGH analysis software measures fluorescence intensity values along the length of the chromosomes and translates the ratios into chromosome profiles (31). The ratio of green to red fluorescence values is used to quantitate genetic imbalances in tumor samples.

Further modification of the CGH technique includes the replacement of metaphase chromosomes with unique DNA sequences spotted in arrays on a glass slide. Fluorescence intensities in both test and reference DNA hybridizations to the immobilized sequences on the array (i.e. cDNA, BAC or oligos) are averaged and normalized, and can be used to calculate an increase or decrease in copy number (32, 33). This array CGH allows for higher resolution of closely spaced genomic aberrations as well as the detection of microdeletions.

Comparative Cytogenetics

Cytogenetic analysis of human tumors reveals a non-random distribution of chromosome rearrangements resulting in genomic imbalances (34). Such aberrations are tissue specific and in some cases are fingerprints for a specific tumor. To better understand the significance of these chromosomal aberrations and identify in a controlled setting those that are early and disease initiating events, animal models of human cancer

are extremely beneficial. The ability to generate gene-specific null mutants in mice affords us the opportunity to elucidate biochemical pathways leading to tumorigenesis and to query the relationship between chromosomal aberrations and the consequences of gene mutation on genomic stability. In addition, the generation of mouse strains hetero- or homozygously deficient for individual genes, the use of conditional knockouts, and

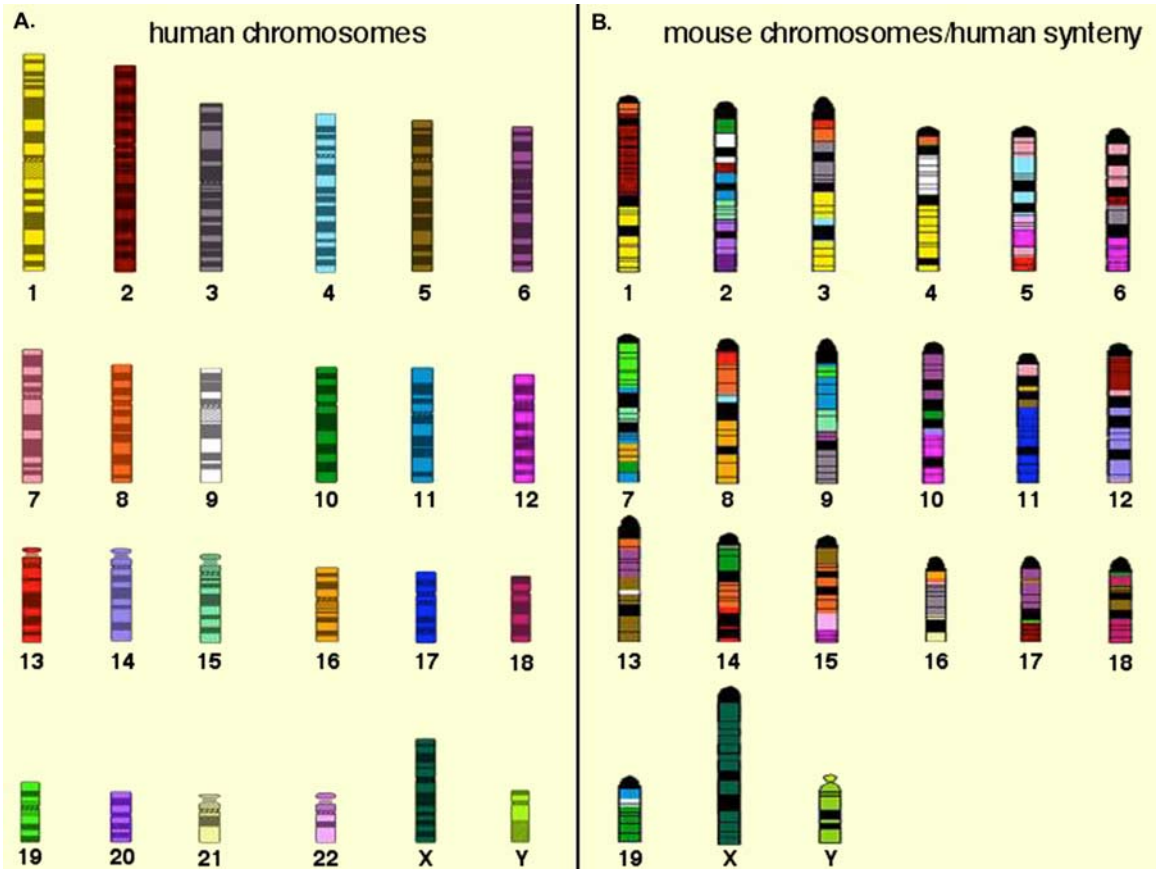

Figure 4: Orthology map of human and mouse chromosomes.

Orthology map of human and mouse chromosomes. (A) Each chromosome in the human ideogram is represented by a single unique color. (B) Every mouse chromosome (except the sex chromosomes) is comprised of regions from different human chromosomes. The regions of orthology can be identified by comparison of their color with the human ideogram in Panel A. Thus, during evolution mouse chromosome 1 has been redistributed to form portions of human chromosomes 8, 2 and 1.

inducible systems for transiently repressing or activating target genes increases the value of mouse models, particularly for cancer (35-38). Because the cytogenetic abnormalities observed in human cancers are fundamental, and often distinguishing features, it is extremely useful to evaluate whether the patterns of genomic imbalances are similar in

human tumors and their corresponding mouse models. The application of molecular cytogenetic techniques, such as SKY and CGH, has been a key factor in identifying similarities between human diseases and their respective mouse models. Mammary cancer is just one such example (39, 40).

The construction of human-mouse orthology maps and the sequencing of both genomes (41, 42) has greatly aided the process of comparative cytogenetics. For example, humans have 22 autosome pairs that vary greatly in size and most have two visible arms (p & q) separated by a centromere (Figure 1A). Mice, however, have 19 autosome pairs of relatively similar size with one arm and a centromere near the end (Figure 1B). Specific chromosomes or chromosome regions of one species can be mapped onto the chromosomes of different species, making it possible to follow chromosome reshuffling during evolution (Figure 4) (43). For instance, mouse chromosome 11 contains sequences orthologous to human chromosome 17, as well as regions of synteny with human 2p (red), 5q (gold), 7p (light pink), 16p (orange) and 22q (dark pink) (Fig 5). By following this comparative cytogenetic approach, we can evaluate chromosome gains and losses in similar tumor types from different species to

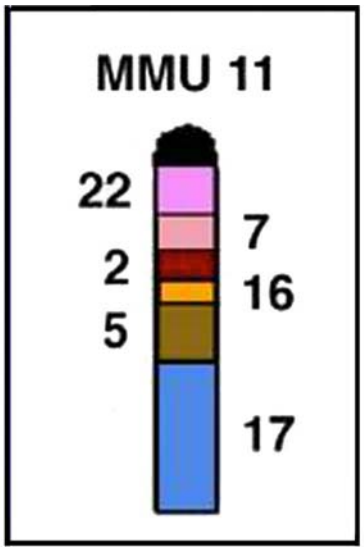

Figure 5: Synteny between mouse chromosome 11 (MMU11) and human chromosome 17 (HSA17).

Synteny between mouse chromosome 11 (MMU11) and human chromosome 17(HSA17). Mouse chromosome 11 contains portions of human chromosomes 22,7,2,16,5 and the entire chromosome 17.

determine if the same set of oncogenes or tumor suppressor genes is amplified or lost, respectively. Because genomic imbalances, generated primarily through chromosomal translocations or aneuploidies, are specific to each type of human malignancy, comparative analyses provides a validation of murine models and an entry point for the identification of new genes involved in tumorigenesis.

Cytogenetic Analysis of Mouse Models of Haematopoietic Malignancies

Haematopoietic malignancies are quite distinct from solid tumors in that rather than gross chromosomal aneuploidy, the causative genomic alterations tend to result from the specific juxtaposition of genes or gene segments at the site of translocations. We have analyzed pro-B cell lymphomas, plasmacytomas and thymic lymphomas from a variety of different mouse models. In mice deficient for the gene mutated in ataxia telangiectasia (ATM) thymic lymphomas develop in nearly all of the animals between 2 and 4 months of age. These tumors exhibit a variety of chromosomal aberrations, including translocations, insertions, deletions, and duplications. Through the use of locus-specific BAC clones, we were able to determine that the breakpoint on chromosome 14 occurs at the T-cell receptor (Tcr) α/δ locus during the programmed genomic recombination process known as V(D)J recombination (44). Other common aberrations included a deletion of the distal portion of chromosome 12 resulting in loss of the immunoglobulin heavy chain gene (IgH) as well as trisomy of chromosome 15, which contains the c-myc oncogene. Aberrations involving the T-cell receptor locus are also found in human ataxia telangiectasia patients and support the use of the *Atm* mouse as a model for tumorigenesis in the absence of this gene product.

Mice deficient in Ku80, a protein involved in the non-homologous end joining (NHEJ) repair of DNA double strand breaks, also develop thymic lymphomas, but at a low frequency. These tumors almost invariably contain extra copies of chromosome 15 (45). When these, and mice deficient in other NHEJ proteins, are crossed onto a p53-deficient background, 100% of the mice now develop tumors, the spectrum of which shifts from T-cell to pro-B cell lymphoma (46-48). These tumors all harbor translocations involving chromosome 12 and 15 resulting in the juxtaposition and co-amplification of the IgH enhancer and the c-myc oncogene. While this rearrangement on

the surface resembled that seen in human Burkitt's lymphoma, whereby the IgH enhancer and c-myc are also brought into close proximity, closer examination of the breakpoints in the mice revealed that the mechanism of translocation in these animals is quite distinct from that observed in the human disease and more closely reflects the type of aberrations (i.e. non-reciprocal translocations, gene amplification and complex chromosome rearrangements) often seen in the solid tumors (45, 49).

Another mouse model, which perhaps more closely mimics human Burkitt's lymphoma or multiple myeloma, is the induction of plasmacytomas in specific mouse strains (50, 51). In this system the rearrangements are believed to occur primarily in mature B-cells during the activation induced deaminase (AID)-dependent process of class switch recombination, not during V(D)J-mediated antigen receptor rearrangement in developing B-cells. The rearrangements involving the IgH locus on chromosome 12 and the c-myc locus on chromosome 15 are typically reciprocal in nature. However, in some instances amplification of the juxtaposed IgH & c-myc loci have been observed (52). Additionally, other differences are evident between this mouse model and the human diseases (53, 54).

Often in human haematopoietic malignancies, translocations result in the joining of two different genes and the production of fusion proteins. Mouse models have been developed in which the fusion protein is introduced as a transgene (for review see (55)). Such mice are extremely useful for studying the effects of expression of these chimeric molecules during the earliest stages of tumorigenesis. Identification of functional elements within the fusion proteins has been achieved through the introduction of transgenes in which various regions have been modified. Thus, the use of mouse models for the study of human haematopoietic malignancies has proven to be extremely fruitful.

Cytogenetic Analysis of Mouse Models of Breast Cancer

Human breast carcinomas are defined by copy number increases frequently mapping to chromosomes 1q, 8q, 17q and 20q where a variety of oncogenes involved in breast cancer have been identified (56, 57). With this knowledge in hand, we applied SKY and CGH to the analysis of primary mammary tumors arising in knock-out mice of the tumor suppressor gene Brca1, mice transgenic for the oncogenes c-Myc or

HER2/Neu, and mice expressing the polyoma virus middle T antigen or the SV40 large T antigen under control of the mammary gland tissue specific promoter MMTV (39, 40, 58). The distribution of gains and losses in each system revealed recurrent patterns of chromosomal aberrations, although each model was quite distinct. The Brca1 KO, however, contained aberrations more consistent with the rearrangements observed in human breast carcinomas.

The major imbalance observed in 58% of the HER2/Neu transgenic mouse tumors was deletion of chromosome 4 (MMU4) bands C-E. This suggested that in addition to HER2/Neu overexpression, decreased expression of a gene(s) in this region of

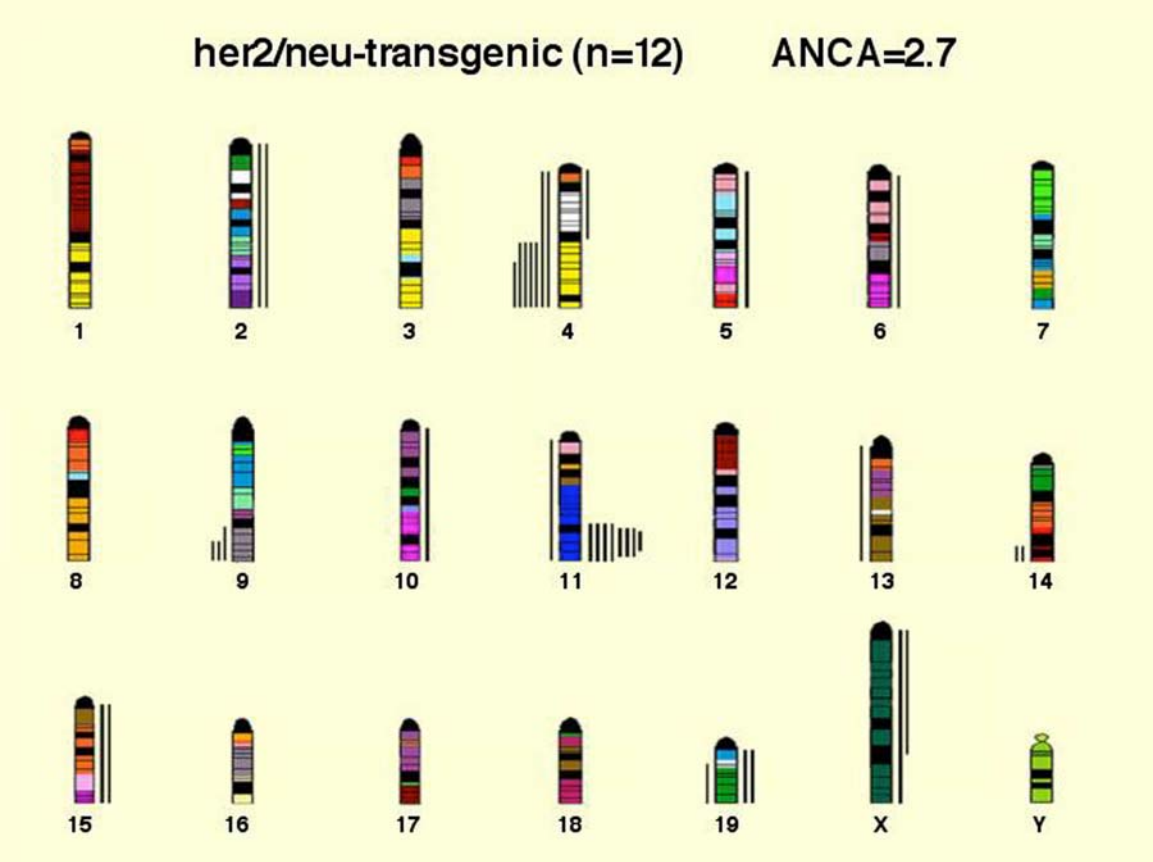

Figure 6: Chromosome gains and losses in the Her2/Neu transgenic mouse model

Chromosome gains and losses in the Her2/Neu transgenic mouse model.
CGH analysis reveals a deletion of chromosome four in the C-E band region as the major imbalance observed in this model. Either complete loss or reduced expression of a gene(s) present in this region of chromosome 4 may therefore be necessary for the induction of mammary gland transformation in the presence of Her2/Neu overexpression.

chromosome 4 was important for the induction of mammary gland transformation (Figure 6). The distal portion of mouse chromosome 4 is orthologous to human 1p31-36 and 9p21, the latter of which contains the INK4 locus. In both the HER2/Neu and the C3(1)SV40Tag models, oncogene amplification results from the presence of acentric extra chromosomal fragments known as double minute chromosomes (dmin) (59, 60). Dmin play a critical role in tumor cell genetics where they are frequently associated with the overexpression of oncogene products (60-65). FISH using locus specific probes revealed that amplification of the HER2/Neu and K-Ras oncogenes was manifested as dmin in the HER2/Neu and C3(1)SV40Tag mouse models, respectively (Figure 7). This finding suggests that in addition to the presence of a strong initial stimulus for cellular transformation (i.e. the overexpression of an oncogene or the presence of a viral protein), secondary genetic alterations are necessary for tumor formation, at least in the mammary gland. These results are consistent with the proposed step-wise increase in chromosome aberrations that parallels tumorigenic progression in human colorectal (66, 67) and cervical carcinomas (29, 56, 68-70).

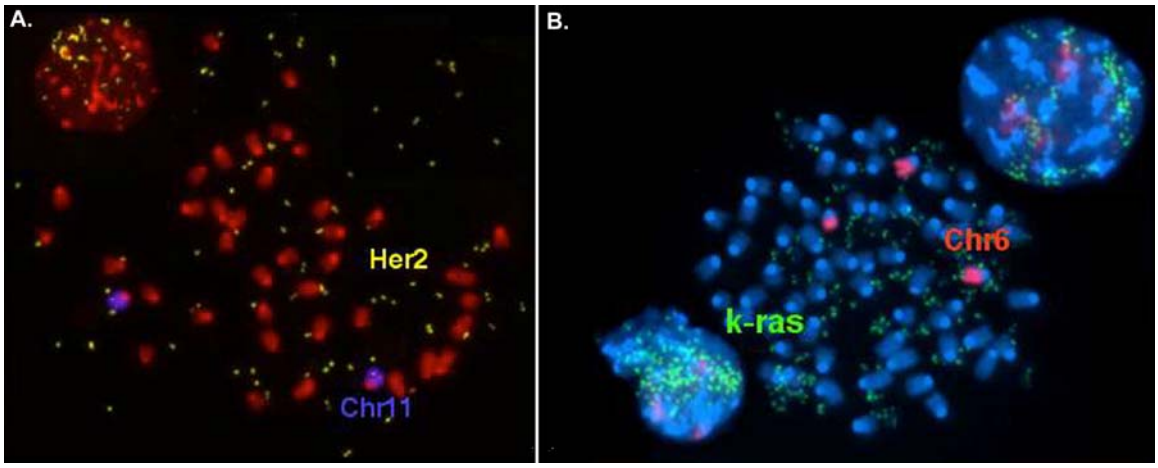

Figure 7: Double minute (dmin) chromosomes in metaphase and interphase cells from Her2/Neu and SV40 C3(1)Tag transgenic mice

(A) In the Her2/Neu transgenic mouse model, dmin chromosomes contain sequences of the Her2/Neu oncogene as demonstrated by hybridization of a locus specific BAC clone (yellow). In blue are shown the two copies of MMU11 (blue) containing the normal mapping position of the oncogene. (B) In the SV40 C3(1)/Tag mouse model, the K-ras oncogene (green) is amplified in the form of double minute chromosomes. The endogenous locus is on MMU6 (red).

A comparison of chromosomal alterations between mouse models and their human tumor counterparts enables further refinement of those regions necessary for tumorigenesis. For example, the region most commonly gained in mammary tumors is the distal portion of chromosome 11. This region is orthologous to an area of the human genome (17q25) amplified in human breast cancer as well as other types of epithelial tumors (34, 71). The tumor suppressor genes BRCA1 and Trp53, as well as the oncogenes HER2/Neu, Tbx2, Rad51c and Grb2 are located in MMU11C-E (72) and human 17q25. However, because the oncogenes in the mouse map closer to the centromere and are outside the region of amplification, we conclude that they are not responsible for tumorigenesis in the mouse, and therefore unlikely to be involved in human breast cancer development. Thus, another candidate gene(s) with oncogenic potential residing on human chromosome 17 may be important for mammary gland transformation.

Our results indicate that cytogenetic experiments conducted in mice with the use of comparative maps are an important tool for understanding the sequence of genetic events required for tumorigenesis. The results obtained can be used to better understand the processes involved in cellular transformation and for the identification of molecular pathways conserved between mice and humans. Increasing the cytogenetic resolution is extremely useful not only for describing genetic alterations, but also for defining those genomic changes that are specific to each tumor type. This has largely been made possible through the combined application of CGH (for identifying regions of gain and loss) and SKY (to identify the mechanism by which the regional copy number or gene expression is altered). We believe that further sub-classification of tumors into more specific categories based on their genomic profile may prove useful in tailoring or identifying responsiveness to particular therapies.

References

1. Solomon, E., Borrow, J., and Goddard, A. D. Chromosome aberrations and cancer. Science, *254:* 1153-1160, 1991.
2. Savage, J. R. K. An Introduction to Chromosomal Aberrations. Atlas Genet Cytogenet Oncol Haematol, March 1999.
3. Cuneo, A. Classification of B-cell non-Hodgkin's lymphomas (NHL): cytogenetic entities, immunopheneotype and clinical features. Atlas Genet Cytogenet Oncol Haematol, February 2000.
4. Yuille, M. Familial chronic lymphocytic leukaemia. Atlas Genet Cytogenet Oncol Haematol, October 1999.
5. Cuneo, A. Classification of B-cell chronic lymphoproliferative disorders (CLD): cytogenetic entities, immunopheneotype and clinical features. Atlas Genet Cytogenet Oncol Haematol, February 2000.
6. Cytogenetic / Clinical Entities in Haematology. Atlas Genet Cytogenet Oncol Haematol.
7. Taub, R., Kirsch, I., Morton, C., Lenoir, G., Swan, D., Tronick, S., Aaronson, S., and Leder, P. Translocation of the c-myc gene into the immunoglobulin heavy chain locus in human Burkitt lymphoma and murine plasmacytoma cells. Proc Natl Acad Sci U S A, *79:* 7837-7841, 1982.
8. Potter, M. and Wiener, F. Plasmacytomagenesis in mice: model of neoplastic development dependent upon chromosomal translocations. Carcinogenesis, *13:* 1681-1697., 1992.
9. Rabbitts, T. H., Baer, R., Davis, M., Forster, A., Rabbitts, P. H., and Malcolm, S. c-myc Gene activation and chromosomal translocation. J Cell Sci Suppl, *1:* 95-101, 1984.
10. Shteper, P. J. and Ben-Yehuda, D. Molecular evolution of chronic myeloid leukaemia. Semin Cancer Biol, *11:* 313-323., 2001.
11. Druker, B. J., Sawyers, C. L., Kantarjian, H., Resta, D. J., Reese, S. F., Ford, J. M., Capdeville, R., and Talpaz, M. Activity of a specific inhibitor of the BCR-ABL tyrosine kinase in the blast crisis of chronic myeloid leukemia and acute lymphoblastic leukemia with the Philadelphia chromosome. N Engl J Med, *344:* 1038-1042., 2001.
12. Heim, S. and Mitelman, F. Cancer Cytogenetics: Wiley-Liss,, 1995.
13. Difilippantonio, M. J. and Ried, T. (eds.) Technicolor Genome Analysis, 1 edition, Vol. 7 (DNA Technology), p. 329. New York: Kluwer Academic/Plenum Publishers, 2003.
14. Kallioniemi, A., Kallioniemi, O.-P., Sudar, D., Rutovitz, D., Gray, J. W., Waldman, F., and Pinkel, D. Comparative genomic hybridization for molecular cytogenetic analysis of solid tumors. Science, *258:* 818-821, 1992.
15. Liyanage, M., Coleman, A., du Manoir, S., Veldman, T., McCormack, S., Dickson, R. B., Barlow, C., Wynshaw-Boris, A., Janz, S., Wienberg, J., Ferguson-Smith, M. A., Schrock, E., and Ried, T. Multicolour spectral karyotyping of mouse chromosomes. Nat Genet, *14:* 312-315, 1996.
16. Schröck, E., du Manoir, S., Veldman, T., Schoell, B., Wienberg, J., Ferguson-Smith, M. A., Ning, Y., Ledbetter, D. H., Bar-Am, I., Soenksen, D., Garini, Y., and Ried, T. Multicolor spectral karyotyping of human chromosomes. Science, *273:* 494-497, 1996.
17. Speicher, M. R., Ballard, S. G., and Ward, D. C. Karyotyping human chromosomes by combinatorial multi-fluor FISH. Nat Genet, *12:* 368-375, 1996.
18. Jentsch, I., Adler, I. D., Carter, N. P., and Speicher, M. R. Karyotyping mouse chromosomes by multiplex-FISH (M-FISH). Chromosome Res, *9:* 211-214, 2001.

19. Veldman, T., Vignon, C., Schrock, E., Rowley, J. D., and Ried, T. Hidden chromosome abnormalities in haematological malignancies detected by multicolour spectral karyotyping. Nat Genet, *15:* 406-410., 1997.
20. Telenius, H., Pelear, A. H., Tunnacliffe, A., Carter, N. P., Behmel, A., Ferguson-Smith, M. A., Nordenskjöld, M., Pfragner, R., and Ponder, B. A. J. Cytogenetic analysis by chromosome painting using DOP-PCR amplified flow sorted chromosomes. Genes Chromosom.Cancer, *4:* 267-263, 1992.
21. Telenius, H., Carter, N. P., Bebb, C. E., Norednskjöld, M., Ponder, B. A. J., and Tunnacliffe, A. Degenerate oligonucleotide-primed PCR (DOP-PCR): general amplification of target DNA by a single degenerate primer. Genomics, *13:* 718-725, 1992.
22. Garini, Y., Gil, A., Bar-Am, I., Cabib, D., and Katzir, N. Signal to Noise Analysis of Multiple Color Fluorescence Imaging Microscopy. Cytometry, *35:* 214-226, 1999.
23. Knutsen, T. and Ried, T. SKY: A comprehensive diagnostoc and research tool. A review of the first 300 published cases. The Journal of the Association of Genetic Technologists, *26:* 3-15, 2000.
24. Hilgenfeld, E., Montagna, C., Padilla-Nash, H., Stapleton, L., Heselmeyer-Haddad, K., and Ried, T. Spectral karyotyping in cancer cytogenetics. Methods Mol Med, *68:* 29-44, 2002.
25. Kallioniemi, O.-P., Kallioniemi, A., Sudar, D., Rutovitz, D., Gray, J. W., Waldman, F., and Pinkel, D. Comparative genomic hybridization: a rapid new method for detecting and mapping DNA amplification in tumors. Sem.Cancer Biol., *4:* 41-46, 1993.
26. Jeuken, J. W., Sprenger, S. H., and Wesseling, P. Comparative genomic hybridization: practical guidelines. Diagn Mol Pathol, *11:* 193-203., 2002.
27. Forozan, F., Karhu, R., Kononen, J., Kallioniemi, A., and Kallioniemi, O. P. Genome screening by comparative genomic hybridization. Trends Genet, *13:* 405-409, 1997.
28. Speicher, M. R., du Manoir, S., Schrock, E., Holtgreve-Grez, H., Schoell, B., Lengauer, C., Cremer, T., and Ried, T. Molecular cytogenetic analysis of formalin-fixed, paraffin-embedded solid tumors by comparative genomic hybridization after universal DNA-amplification. Hum Mol Genet, *2:* 1907-1914., 1993.
29. Heselmeyer, K., Schrock, E., du Manoir, S., Blegen, H., Shah, K., Steinbeck, R., Auer, G., and Ried, T. Gain of chromosome 3q defines the transition from severe dysplasia to invasive carcinoma of the uterine cervix. Proc Natl Acad Sci U S A, *93:* 479-484., 1996.
30. du Manoir, S., Schrock, E., Bentz, M., Speicher, M. R., Joos, S., Ried, T., Lichter, P., and Cremer, T. Quantitative analysis of comparative genomic hybridization. Cytometry, *19:* 27-41, 1995.
31. Piper, J., Rutovitz, D., Sudar, D., Kallioniemi, A., Kallioniemi, O.-P., Waldman, F., Gray, J., and Pinkel, D. Computer image analysis of comparative genomic hybridization. Cytometry, *19:* 10-26, 1995.
32. Pinkel, D., Segraves, R., Sudar, D., Clark, S., Poole, I., Kowbel, D., Collins, C., Kuo, W. L., Chen, C., Zhai, Y., Dairkee, S. H., Ljung, B. M., Gray, J. W., and Albertson, D. G. High resolution analysis of DNA copy number variation using comparative genomic hybridization to microarrays. Nat Genet, *20:* 207-211, 1998.
33. Hyman, E., Kauraniemi, P., Hautaniemi, S., Wolf, M., Mousses, S., Rozenblum, E., Ringner, M., Sauter, G., Monni, O., Elkahloun, A., Kallioniemi, O. P., and Kallioniemi, A. Impact of DNA amplification on gene expression patterns in breast cancer. Cancer Res, *62:* 6240-6245, 2002.
34. Ried, T., Just, K. E., Holtgreve-Grez, H., du Manoir, S., Speicher, M. R., Schrock, E., Latham, C., Blegen, H., Zetterberg, A., Cremer, T., and Auer, G. Comparative genomic hybridization of formalin-fixed, paraffin-embedded breast tumors reveals different

patterns of chromosomal gains and losses in fibroadenomas and diploid and aneuploid carcinomas. Cancer Res, *55:* 5415-5423, 1995.

35. Herzig, M. and Christofori, G. Recent advances in cancer research: mouse models of tumorigenesis. Biochim Biophys Acta, *1602:* 97-113, 2002.
36. Weiss, B. and Shannon, K. Mouse cancer models as a platform for performing preclinical therapeutic trials. Curr Opin Genet Dev, *13:* 84-89, 2003.
37. Hunter, K. W. and Williams, R. W. Complexities of cancer research: mouse genetic models. Ilar J, *43:* 80-88, 2002.
38. Marx, J. Medicine. Building better mouse models for studying cancer. Science, *299:* 1972-1975, 2003.
39. Montagna, C., Andrechek, E. R., Padilla-Nash, H., Muller, W. J., and Ried, T. Centrosome abnormalities, recurring deletions of chromosome 4, and genomic amplification of HER2/neu define mouse mammary gland adenocarcinomas induced by mutant HER2/neu. Oncogene, *21:* 890-898, 2002.
40. Weaver, Z., Montagna, C., Xu, X., Howard, T., Gadina, M., Brodie, S. G., Deng, C. X., and Ried, T. Mammary tumors in mice conditionally mutant for Brca1 exhibit gross genomic instability and centrosome amplification yet display a recurring distribution of genomic imbalances that is similar to human breast cancer. Oncogene, *21:* 5097-5107, 2002.
41. Waterston, R. H., Lindblad-Toh, K., Birney, E., Rogers, J., Abril, J. F., Agarwal, P., Agarwala, R., Ainscough, R., Alexandersson, M., An, P., Antonarakis, S. E., Attwood, J., Baertsch, R., Bailey, J., Barlow, K., Beck, S., Berry, E., Birren, B., Bloom, T., Bork, P., Botcherby, M., Bray, N., Brent, M. R., Brown, D. G., Brown, S. D., Bult, C., Burton, J., Butler, J., Campbell, R. D., Carninci, P., Cawley, S., Chiaromonte, F., Chinwalla, A. T., Church, D. M., Clamp, M., Clee, C., Collins, F. S., Cook, L. L., Copley, R. R., Coulson, A., Couronne, O., Cuff, J., Curwen, V., Cutts, T., Daly, M., David, R., Davies, J., Delehaunty, K. D., Deri, J., Dermitzakis, E. T., Dewey, C., Dickens, N. J., Diekhans, M., Dodge, S., Dubchak, I., Dunn, D. M., Eddy, S. R., Elnitski, L., Emes, R. D., Eswara, P., Eyras, E., Felsenfeld, A., Fewell, G. A., Flicek, P., Foley, K., Frankel, W. N., Fulton, L. A., Fulton, R. S., Furey, T. S., Gage, D., Gibbs, R. A., Glusman, G., Gnerre, S., Goldman, N., Goodstadt, L., Grafham, D., Graves, T. A., Green, E. D., Gregory, S., Guigo, R., Guyer, M., Hardison, R. C., Haussler, D., Hayashizaki, Y., Hillier, L. W., Hinrichs, A., Hlavina, W., Holzer, T., Hsu, F., Hua, A., Hubbard, T., Hunt, A., Jackson, I., Jaffe, D. B., Johnson, L. S., Jones, M., Jones, T. A., Joy, A., Kamal, M., Karlsson, E. K., Karolchik, D., Kasprzyk, A., Kawai, J., Keibler, E., Kells, C., Kent, W. J., Kirby, A., Kolbe, D. L., Korf, I., Kucherlapati, R. S., Kulbokas, E. J., Kulp, D., Landers, T., Leger, J. P., Leonard, S., Letunic, I., Levine, R., Li, J., Li, M., Lloyd, C., Lucas, S., Ma, B., Maglott, D. R., Mardis, E. R., Matthews, L., Mauceli, E., Mayer, J. H., McCarthy, M., McCombie, W. R., McLaren, S., McLay, K., McPherson, J. D., Meldrim, J., Meredith, B., Mesirov, J. P., Miller, W., Miner, T. L., Mongin, E., Montgomery, K. T., Morgan, M., Mott, R., Mullikin, J. C., Muzny, D. M., Nash, W. E., Nelson, J. O., Nhan, M. N., Nicol, R., Ning, Z., Nusbaum, C., O'Connor, M. J., Okazaki, Y., Oliver, K., Overton-Larty, E., Pachter, L., Parra, G., Pepin, K. H., Peterson, J., Pevzner, P., Plumb, R., Pohl, C. S., Poliakov, A., Ponce, T. C., Ponting, C. P., Potter, S., Quail, M., Reymond, A., Roe, B. A., Roskin, K. M., Rubin, E. M., Rust, A. G., Santos, R., Sapojnikov, V., Schultz, B., Schultz, J., Schwartz, M. S., Schwartz, S., Scott, C., Seaman, S., Searle, S., Sharpe, T., Sheridan, A., Shownkeen, R., Sims, S., Singer, J. B., Slater, G., Smit, A., Smith, D. R., Spencer, B., Stabenau, A., Stange-Thomann, N., Sugnet, C., Suyama, M., Tesler, G., Thompson, J., Torrents, D., Trevaskis, E., Tromp, J., Ucla, C., Ureta-Vidal, A., Vinson, J. P., Von Niederhausern, A. C., Wade, C. M., Wall, M., Weber, R. J., Weiss, R. B., Wendl, M. C., West, A. P., Wetterstrand, K., Wheeler, R., Whelan, S., Wierzbowski, J., Willey,

D., Williams, S., Wilson, R. K., Winter, E., Worley, K. C., Wyman, D., Yang, S., Yang, S. P., Zdobnov, E. M., Zody, M. C. and Lander, E. S. Initial sequencing and comparative analysis of the mouse genome. Nature, *420:* 520-562, 2002.

42. Okazaki, Y., Furuno, M., Kasukawa, T., Adachi, J., Bono, H., Kondo, S., Nikaido, I., Osato, N., Saito, R., Suzuki, H., Yamanaka, I., Kiyosawa, H., Yagi, K., Tomaru, Y., Hasegawa, Y., Nogami, A., Schonbach, C., Gojobori, T., Baldarelli, R., Hill, D. P., Bult, C., Hume, D. A., Quackenbush, J., Schriml, L. M., Kanapin, A., Matsuda, H., Batalov, S., Beisel, K. W., Blake, J. A., Bradt, D., Brusic, V., Chothia, C., Corbani, L. E., Cousins, S., Dalla, E., Dragani, T. A., Fletcher, C. F., Forrest, A., Frazer, K. S., Gaasterland, T., Gariboldi, M., Gissi, C., Godzik, A., Gough, J., Grimmond, S., Gustincich, S., Hirokawa, N., Jackson, I. J., Jarvis, E. D., Kanai, A., Kawaji, H., Kawasawa, Y., Kedzierski, R. M., King, B. L., Konagaya, A., Kurochkin, I. V., Lee, Y., Lenhard, B., Lyons, P. A., Maglott, D. R., Maltais, L., Marchionni, L., McKenzie, L., Miki, H., Nagashima, T., Numata, K., Okido, T., Pavan, W. J., Pertea, G., Pesole, G., Petrovsky, N., Pillai, R., Pontius, J. U., Qi, D., Ramachandran, S., Ravasi, T., Reed, J. C., Reed, D. J., Reid, J., Ring, B. Z., Ringwald, M., Sandelin, A., Schneider, C., Semple, C. A., Setou, M., Shimada, K., Sultana, R., Takenaka, Y., Taylor, M. S., Teasdale, R. D., Tomita, M., Verardo, R., Wagner, L., Wahlestedt, C., Wang, Y., Watanabe, Y., Wells, C., Wilming, L. G., Wynshaw-Boris, A., Yanagisawa, M., Yang, I., Yang, L., Yuan, Z., Zavolan, M., Zhu, Y., Zimmer, A., Carninci, P., Hayatsu, N., Hirozane-Kishikawa, T., Konno, H., Nakamura, M., Sakazume, N., Sato, K., Shiraki, T., Waki, K., Kawai, J., Aizawa, K., Arakawa, T., Fukuda, S., Hara, A., Hashizume, W., Imotani, K., Ishii, Y., Itoh, M., Kagawa, I., Miyazaki, A., Sakai, K., Sasaki, D., Shibata, K., Shinagawa, A., Yasunishi, A., Yoshino, M., Waterston, R., Lander, E. S., Rogers, J., Birney, E. and Hayashizaki, Y. Analysis of the mouse transcriptome based on functional annotation of 60,770 full-length cDNAs. Nature, *420:* 563-573, 2002.
43. O'Brien, S. J., Menotti-Raymond, M., Murphy, W. J., Nash, W. G., Wienberg, J., Stanyon, R., Copeland, N. G., Jenkins, N. A., Womack, J. E., and Marshall Graves, J. A. The promise of comparative genomics in mammals. Science, *286:* 458-462, 479-481., 1999.
44. Liyanage, M., Weaver, Z., Barlow, C., Coleman, A., Pankratz, D. G., Anderson, S., Wynshaw-Boris, A., and Ried, T. Abnormal rearrangement within the alpha/delta T-cell receptor locus in lymphomas from Atm-deficient mice. Blood, *96:* 1940-1946., 2000.
45. Difilippantonio, M. J., Petersen, S., Chen, H. T., Johnson, R., Jasin, M., Kanaar, R., Ried, T., and Nussenzweig, A. Evidence for replicative repair of DNA double-strand breaks leading to oncogenic translocation and gene amplification. J Exp Med, *196:* 469-480., 2002.
46. Difilippantonio, M. J., Zhu, J., Chen, H. T., Meffre, E., Nussenzweig, M. C., Max, E. E., Ried, T., and Nussenzweig, A. DNA repair protein Ku80 suppresses chromosomal aberrations and malignant transformation. Nature, *404:* 510-514., 2000.
47. Frank, K. M., Sharpless, N. E., Gao, Y., Sekiguchi, J. M., Ferguson, D. O., Zhu, C., Manis, J. P., Horner, J., DePinho, R. A., and Alt, F. W. DNA ligase IV deficiency in mice leads to defective neurogenesis and embryonic lethality via the p53 pathway. Mol Cell, *5:* 993-1002., 2000.
48. Gao, Y., Ferguson, D. O., Xie, W., Manis, J. P., Sekiguchi, J., Frank, K. M., Chaudhuri, J., Horner, J., DePinho, R. A., and Alt, F. W. Interplay of p53 and DNA-repair protein XRCC4 in tumorigenesis, genomic stability and development. Nature, *404:* 897-900., 2000.
49. Zhu, C., Mills, K. D., Ferguson, D. O., Lee, C., Manis, J., Fleming, J., Gao, Y., Morton, C. C., and Alt, F. W. Unrepaired DNA breaks in p53-deficient cells lead to oncogenic gene amplification subsequent to translocations. Cell, *109:* 811-821, 2002.

50. Potter, M. Perspectives on the origins of multiple myeloma and plasmacytomas in mice. Hematol Oncol Clin North Am, *6:* 211-223., 1992.
51. Gado, K., Silva, S., Paloczi, K., Domjan, G., and Falus, A. Mouse plasmacytoma: an experimental model of human multiple myeloma. Haematologica, *86:* 227-236, 2001.
52. Coleman, A. E., Kovalchuk, A. L., Janz, S., Palini, A., and Ried, T. Jumping translocation breakpoint regions lead to amplification of rearranged Myc. Blood, *93:* 4442-4444., 1999.
53. Muller, J. R., Janz, S., and Potter, M. Differences between Burkitt's lymphomas and mouse plasmacytomas in the immunoglobulin heavy chain/c-myc recombinations that occur in their chromosomal translocations. Cancer Res, *55:* 5012-5018., 1995.
54. Muller, J. R., Janz, S., and Potter, M. Illegitimate recombinations between c-myc and immunoglobulin loci are remodeled by deletions in mouse plasmacytomas but not in Burkitt's lymphomas. Curr Top Microbiol Immunol, *194:* 425-429, 1995.
55. Bernardi, R., Grisendi, S., and Pandolfi, P. P. Modelling haematopoietic malignancies in the mouse and therapeutical implications. Oncogene, *21:* 3445-3458, 2002.
56. Ried, T., Heselmeyer-Haddad, K., Blegen, H., Schrock, E., and Auer, G. Genomic changes defining the genesis, progression, and malignancy potential in solid human tumors: a phenotype/genotype correlation. Genes Chromosomes Cancer, *25:* 195-204, 1999.
57. Tirkkonen, M., Tanner, M., Karhu, R., Kallioniemi, A., Isola, J., and Kallioniemi, O. P. Molecular cytogenetics of primary breast cancer by CGH. Genes Chromosomes Cancer, *21:* 177-184., 1998.
58. Weaver, Z. A., McCormack, S. J., Liyanage, M., du Manoir, S., Coleman, A., Schrock, E., Dickson, R. B., and Ried, T. A recurring pattern of chromosomal aberrations in mammary gland tumors of MMTV-cmyc transgenic mice. Genes Chromosomes Cancer, *25:* 251-260, 1999.
59. Alitalo, K. and Schwab, M. Oncogene amplification in tumor cells. Advances in Cancer Research, *47:* 235-281, 1986.
60. Hahn, P. J. Molecular biology of double-minute chromosomes. Bioessays, *15:* 477-484., 1993.
61. Mathew, S., Lorsbach, R. B., Shearer, P., Sandlund, J. T., and Raimondi, S. C. Double minute chromosomes and c-MYC amplification in a child with secondary myelodysplastic syndrome after treatment for acute lymphoblastic leukemia. Leukemia, *14:* 1314-1315, 2000.
62. O'Malley, F., Rayeroux, K., Cole-Sinclair, M., Tong, M., and Campbell, L. J. MYC amplification in two further cases of acute myeloid leukemia with trisomy 4 and double minute chromosomes. Cancer Genet Cytogenet, *109:* 123-125, 1999.
63. Mohamed, A. N., Mahalak, S., Goldfarb, S. B., and Palutke, M. Double minute chromosomes contain amplified c-myc oncogene sequences in acute myeloid leukemia. Hematopathol Mol Hematol, *10:* 193-199, 1996.
64. Karasawa, M., Okamoto, K., Maehara, T., Tsukamoto, N., Morita, K., Naruse, T., and Omine, M. Detection of c-myc oncogene amplification in a CML blastic phase patient with double minute chromosomes. Leuk Res, *20:* 85-91, 1996.
65. Nielsen, J. L., Walsh, J. T., Degen, D. R., Drabek, S. M., McGill, J. R., and von Hoff, D. D. Evidence of gene amplification in the form of double minute chromosomes is frequently observed in lung cancer. Cancer Genet Cytogenet, *65:* 120-124, 1993.
66. Ried, T., Knutzen, R., Steinbeck, R., Blegen, H., Schrock, E., Heselmeyer, K., du Manoir, S., and Auer, G. Comparative genomic hybridization reveals a specific pattern of chromosomal gains and losses during the genesis of colorectal tumors. Genes Chromosomes Cancer, *15:* 234-245, 1996.

67. Tsao, J. L., Tavare, S., Salovaara, R., Jass, J. R., Aaltonen, L. A., and Shibata, D. Colorectal adenoma and cancer divergence. Evidence of multilineage progression. Am J Pathol, *154:* 1815-1824., 1999.
68. Granberg, I. Chromosomes in preinvasive, microinvasive and invasive cervical carcinoma. Hereditas, *68:* 165-218, 1971.
69. Heselmeyer, K., Macville, M., Schrock, E., Blegen, H., Hellstrom, A. C., Shah, K., Auer, G., and Ried, T. Advanced-stage cervical carcinomas are defined by a recurrent pattern of chromosomal aberrations revealing high genetic instability and a consistent gain of chromosome arm 3q. Genes Chromosomes Cancer, *19:* 233-240, 1997.
70. Allen, D. G., White, D. J., Hutchins, A. M., Scurry, J. P., Tabrizi, S. N., Garland, S. M., and Armes, J. E. Progressive genetic aberrations detected by comparative genomic hybridization in squamous cell cervical cancer. Br J Cancer, *83:* 1659-1663, 2000.
71. Mahlamaki, E. H., Barlund, M., Tanner, M., Gorunova, L., Hoglund, M., Karhu, R., and Kallioniemi, A. Frequent amplification of 8q24, 11q, 17q, and 20q-specific genes in pancreatic cancer. Genes Chromosomes Cancer, *35:* 353-358., 2002.
72. Barlund, M., Monni, O., Kononen, J., Cornelison, R., Torhorst, J., Sauter, G., Kallioniemi, O.-P., and Kallioniemi, A. Multiple genes at 17q23 undergo amplification and overexpression in breast cancer. Cancer Res, *60:* 5340-5344., 2000.